On the ferroelastic phase transition in $LiRb_5(SO_4)_3.1.5H_2SO_4$: Brillouin scattering study and theoretical modelling

1989 J. Phys.: Condens. Matter 1 4425

(http://iopscience.iop.org/0953-8984/1/27/015)

J. Phys.: Condens. Matter **1** (1989) 4425–4439. Printed in the UK

On the ferroelastic phase transition in $LiRb_5(SO_4)_3 \cdot 1.5H_2SO_4$: Brillouin scattering study and theoretical modelling

B Mróz†, J A Tuszyński‡, H Kiefte§ and M J Clouter§

† Institute of Physics, A Mickiewicz University, Grunwaldzka 6, 60-780 Poznań, Poland
‡ Department of Physics, University of Alberta, Edmonton, Alberta, Canada T6G 2J1
§ Department of Physics, Memorial University of Newfoundland, St John's, Newfoundland, Canada A1B 3X7

Received 15 June 1988, in final form 25 November 1988

Abstract. High-resolution Brillouin spectroscopy was used to study the elastic properties of ferroelastic $LiRb_5(SO_4)_3 \cdot 1.5H_2SO_4$ (LRSHS). The velocities, linewidths and intensities of 12 acoustic modes were measured in the temperature range from 100 to 300 K. The critical temperature for the 4mm → mm2 transition was found to be approximately 132 K. All non-zero components of the elastic stiffness tensor of the para- and ferroelastic phases were determined. The frequency of the pure transverse mode associated with the c_{66} elastic constant was found to be strongly temperature-dependent in the vicinity of T_c. In order to explain all experimental features a mean-field model was postulated with a free-energy expansion in terms of an order parameter (which drives the transition), spontaneous strain, the remaining strain components and polarisation. It was demonstrated that a coupling term involving spontaneous strain and polarisation appears to be the reason for the observed incomplete softening of the c_{66} mode as $T \rightarrow T_c$. It also appears to agree with the observed crossover from a square-root to a linear dependence of polarisation on temperature. Moreover, coupling between the spontaneous strain and the other strain components results in a weak temperature dependence of the elastic constants c_{ij} $(i, j \neq 6)$, in agreement with experimental observations.

1. Introduction

In the last few years ferroelastic crystals have been the subject of a large number of theoretical and experimental studies because of their interesting physical properties and possible applications (Wadhawan 1982, Cummins 1983, Toledano *et al* 1983). In recent papers we have reported on Brillouin scattering studies of two ferroelastic materials: $LiCsSO_4$ (Mróz *et al* 1987) and $LiKSO_4$ (Mróz *et al* 1989). The objective of this paper is to report Brillouin scattering experiments on a new ferroelastic material, $LiRb_5(SO_4)_3 \cdot 1.5H_2SO_4$ (LRSHS), and to explain the experimental results using mean-field Landau theory involving appropriate thermodynamic variables.

At room temperature, LRSHS belongs to the tetragonal system and has lattice parameters $a = b = 7.740$ Å and $c = 7.442$ Å (Pietraszko 1987). As was recently shown from pyroelectric, dielectric and thermal studies (Wolejko *et al* 1988b), LRSHS undergoes a structural second-order phase transition between two polar point groups at about

0953-8984/89/274425 + 15 $02.50

135 K. The ferroelastic character of this transition was confirmed by direct observation of domain structure reorientable under the action of appropriate mechanical stress (Wolejko *et al* 1988a). Since there was a lack of structural information about LRSHS, we have recently proposed a procedure for determining its low-temperature point group (Mróz *et al* 1988) from the temperature dependences of the Brillouin line shifts of the phonons propagating in the directions of the shear planes [101] and [10$\bar{1}$]. We consequently found that LRSHS undergoes a ferroelastic phase transition from the (high-temperature) tetragonal point group 4mm to the (low-temperature) orthorhombic mm2. It is not possible at this stage to state conclusively whether this is a purely ferroelastic or a pseudo-ferroelastic phase transition, but we tend to favour the latter eventuality.

In the present experiment we have measured the temperature dependences of the frequency shifts and linewidths of the 12 acoustic modes, which allowed us to calculate the temperature changes of all non-zero components of the elastic stiffness tensor of the prototype phase 4mm and the ferroelastic phase mm2. Section 2 details the experimental procedure adopted while § 3 summarises the experimental results found. In § 4 we present a theoretical model based on the mean-field approximation using a Landau-type free-energy expansion involving an order parameter (which drives the transition), spontaneous strain, the remaining strain components and polarisation. Cross-terms that couple spontaneous strain with the other variables, especially polarisation, will be shown to play an important role in explaining the observed behaviour.

2. Experimental procedure

Colourless single crystals of LRSHS were grown isothermally at 310 K from an acid aqueous solution of pH $\leqslant 1$. The exact composition of the crystals was confirmed using nuclear absorption spectroscopy. Samples of three different orientations were prepared in the form of cubes ($5 \times 5 \times 5$ mm^3) to measure the sound velocities along the crystallographic axes and the bisectors of these axes.

The Brillouin spectrometer has been described in detail elsewhere (Ahmad *et al* 1982). The incident light was provided by a stabilised single-mode argon-ion laser (CR-52) operating at $\lambda = 514.5$ nm with an output of about 100 mW polarised perpendicularly to the scattering plane. The scattered light was analysed at 90° with a peizoelectrically scanned triple-pass Fabry–Perot interferometer (Burleigh RC-110) utilising free spectral ranges (FSR) of 25.03 and 16.50 GHz at a finesse of about 60. Spectra were accumulated with a photon-counting data-acquisition and stabilisation system (Burleigh DAS-1).

Sound velocities were calculated from the measured frequency shifts $\Delta\nu$ using the Brillouin equation, which in the case of right-angle scattering geometry takes the form

$$v = \lambda \Delta \nu (n_i^2 + n_s^2)^{-1/2} \tag{1}$$

where λ is the wavelength of the incident light, and n_i and n_s are the refractive indices for the incident and scattered light, respectively. Refractive indices of LRSHS were found, at room temperature, by comparing the crystal samples with several liquids (Cargille Labs) of known refractive indices. We found n_x or $n_y = 1.426$ and $n_z = 1.468 \pm 0.001$. All Brillouin measurements were performed in the temperature range from 100 to 300 K using the cryostat described in a previous publication (Mróz *et al* 1987). The temperature of the sample was regulated with a stability of ± 0.03 K.

3. Experimental results

Table 1 contains expression of ρv^2 as a function of the elastic constants for the tetragonal (4mm) and orthorhombic (mm2) phases using standard notation (Vacher and Boyer 1972). These relations were derived from solutions of the equation of motion (Landau and Lifshitz 1959) for the three acoustic waves propagating in the direction $\boldsymbol{Q}$ given by

$$|c_{ijkl}q_jq_k - \rho v^2\delta_{il}| = 0 \tag{2}$$

where q_j, q_k are direction cosines of $\boldsymbol{Q}$, ρ is the density of the crystal (2.81 g cm^{-3}) and c_{ijkl} are elastic stiffness tensor components.

We have observed 12 of the 18 Brillouin modes listed in table 1. The measured frequency shifts versus temperature for the pure longitudinal (L) and pure transverse (T) modes are plotted in figure 1. We found the frequency shifts of the longitudinal modes γ_1, γ_4 and γ_7 as well as of the pure transverse modes γ_3 and γ_5 to be slightly temperature-dependent whereas the frequency of the pure transverse mode γ_2 was strongly temperature-dependent with frequency shifts from 5.06 GHz at room temperature, to 2.11 GHz at 132 K. The observed temperature behaviour is understood since the appearance of the soft acoustic mode during the 4mm $\rightarrow$ mm2 transition is associated (Toledano *et al* 1983) with the elastic constant c_{66} and is directly related to the γ_2 modes (see table 1). In addition, we observed an increase in relative intensity of this mode together with the broadening of the Brillouin line, as shown in figure 2, after deconvolution with the 0.50 GHz instrumental linewidth.

The temperature dependences of the frequencies of the remaining modes are plotted in figure 3. The temperature behaviour of the γ_{15} and γ_{18} modes was recently reported (Mróz *et al* 1988) and the observed softening may be explained since above the critical temperature T_c ($\simeq$132 K) these modes are related to $\rho v^2 = \frac{1}{2}(c_{44} + c_{66})$. The frequency of the γ_{10} mode is slightly temperature-dependent up to the transition point and increases distinctly in the ferroelastic phase. Quasi-longitudinal modes γ_{13} and γ_{16} show a linear increase in frequency shifts as $T \rightarrow T_c$ and the splitting of their values observed below T_c is understood since for the orthorhombic phase we have $c_{11} \neq c_{22}$, $c_{44} \neq c_{55}$ and $c_{13} \neq c_{23}$. The frequency shift of the γ_{17} quasi-transverse mode increases linearly with decreasing temperature in the entire region studied.

The temperature dependences of the elastic constants calculated for both the para- and ferroelastic phases from the observed shifts of pure L and T modes are plotted in figure 4. The c_{11}, c_{22} and c_{33} elastic constants are essentially temperature-independent and increase with decreasing temperature (as expected). The c_{66} elastic constant is strongly temperature-dependent. The related sound velocity changes from 1270 m s^{-1} at room temperature to 165 m s^{-1} at T_c. It should be emphasised here that c_{66} does not vanish at T_c, signifying an incomplete mode softening, which will be analysed theoretically in § 4. The temperature dependences of the elastic constants c_{12}, c_{13} and c_{23} are plotted in figure 5. The c_{13} elastic constant does not change with temperature in either the para- or ferroelastic phases. The c_{12} component increases slowly as $T \rightarrow T_c$ and exhibits a strong temperature dependence ('hardening') in the ferroelastic phase. The solutions of $\rho v^2(c_{ij})$ for the γ_{10} (below T_c), γ_{13} and γ_{16} modes give two sets of values for c_{12}, c_{13} and c_{23}. We discard the incorrect determinations of these components by checking the consistency of the velocity extrema in the pure mode directions (Vacher *et al* 1972, Brugger 1965). In table 2 we list the precise values of all non-zero elastic constants at 300, 132 and 100 K.

Table 1. The ρv^2 as a function of the elastic constants in the tetragonal (4mm) and orthorhombic (mm2) phases.

Phonon	Mode[a]	4mm phase	mm2 phase
[100]	L γ_1*	c_{11}	c_{11}
	T γ_2*	c_{66}	c_{66}
	T γ_3*	c_{44}	c_{55}
[010]	L γ_4*	c_{11}	c_{22}
	T γ_5*	c_{44}	c_{44}
	T γ_6	c_{66}	c_{66}
[001]	L γ_7*	c_{33}	c_{33}
	T γ_8	c_{44}	c_{55}
	T γ_9	c_{44}	c_{44}
[110]	L γ_{10}*	$\frac{1}{2}[c_{11} + c_{66} + (c_{12} + c_{66})]$	$\frac{1}{4}(c_{11} + c_{22} + 2c_{66} + [(c_{11} - c_{22})^2 + 4(c_{12} + c_{66})^2]^{1/2})$
	T γ_{11}	$\frac{1}{2}[c_{11} + c_{66} - (c_{12} + c_{66})]$	$\frac{1}{4}(c_{11} + c_{22} + 2c_{66} - [(c_{11} - c_{22})^2 + 4(c_{12} + c_{66})^2]^{1/2})$
	T γ_{12}	c_{44}	$\frac{1}{2}(c_{44} + c_{55})$
[101]	L γ_{13}*	$\frac{1}{4}(c_{11} + c_{33} + 2c_{44} + [(c_{33} - c_{11})^2 + 4(c_{13} + c_{44})^2]^{1/2})$	$\frac{1}{4}(c_{11} + c_{33} + 2c_{55} + [(c_{11} - c_{33})^2 + 4(c_{13} + c_{55})^2]^{1/2})$
	T γ_{14}	$\frac{1}{4}(c_{11} - c_{33} + 2c_{44} - [(c_{33} - c_{11})^2 + 4(c_{13} + c_{44})^2]^{1/2})$	$\frac{1}{4}(c_{11} + c_{33} + 2c_{55} - [(c_{11} - c_{33})^2 + 4(c_{13} + c_{55})^2]^{1/2})$
	T γ_{15}*	$\frac{1}{4}(c_{44} + c_{66})$	$\frac{1}{2}(c_{44} + c_{66})$
[011]	L γ_{16}*	$\frac{1}{4}(c_{11} + c_{33} + 2c_{44} + [(c_{33} - c_{11})^2 + 4(c_{13} + c_{44})^2]^{1/2})$	$\frac{1}{4}(c_{22} + c_{33} + 2c_{44} + [(c_{33} - c_{22})^2 + 4(c_{23} + c_{44})^2]^{1/2})$
	T γ_{17}*	$\frac{1}{4}(c_{11} + c_{33} + 2c_{44} - [(c_{33} - c_{11})^2 + 4(c_{13} + c_{44})^2]^{1/2})$	$\frac{1}{4}(c_{22} + c_{33} + 2c_{44} - [(c_{33} - c_{22})^2 + 4(c_{23} + c_{44})^2]^{1/2})$
	T γ_{18}*	$\frac{1}{4}(c_{44} + c_{66})$	$\frac{1}{4}(c_{55} + c_{66})$

[a] Asterisks (*) indicate which modes were observed in our experiment.

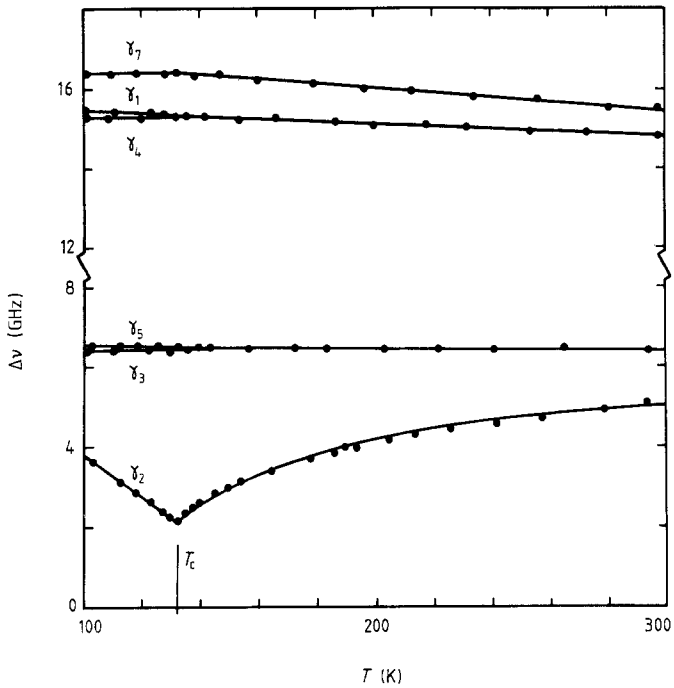

Figure 1. Temperature dependence of the Brillouin shifts for the pure longitudinal (L) and pure transverse (T) modes γ_i ($i = 1, 2, 3, 4, 5, 7$).

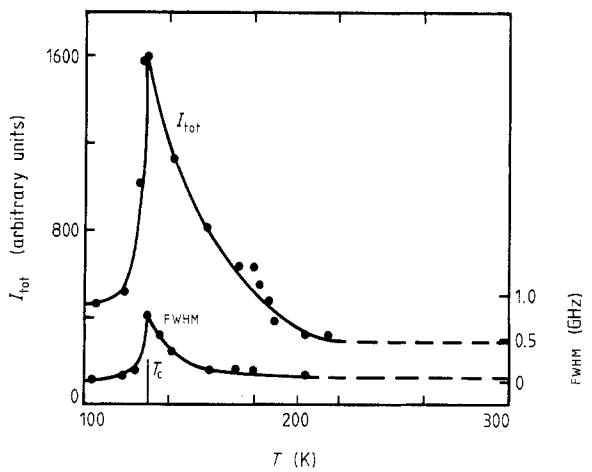

Figure 2. Temperature dependence of the full width at half-maximum (FWHM) and the integrated intensity I_{tot} of the γ_2 soft mode.

As is well known, the elastic constants measured by the Brillouin scattering technique correspond to the adiabatic conditions and electric neutrality, whereas the mean-field approximation (as applied in the present paper) refers to the isothermal elastic constants at a constant electric field. Thus, it was necessary to evaluate the piezoelastic and isothermal–adiabatic corrections. We find that only the c_{44} and c_{55} elastic constants can

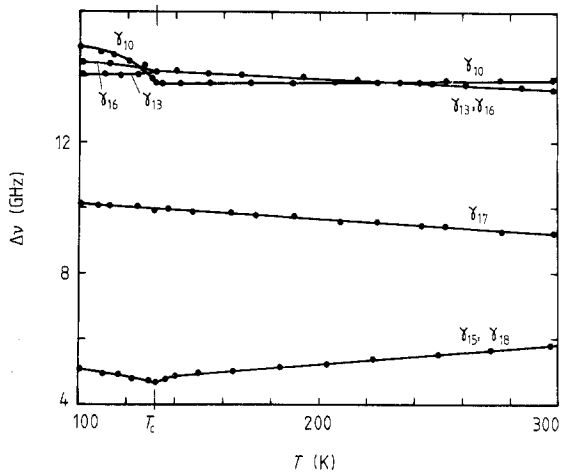

Figure 3. Temperature dependence of the Brillouin shifts for quasi-longitudinal (QL) and quasi-transverse (QT) modes γ_i (i = 10, 13, 15, 16, 17, 18).

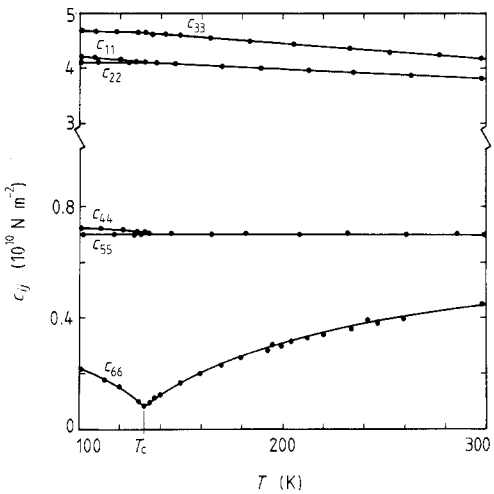

Figure 4. Elastic constants c_{ij} related to the pure modes plotted as a function of temperature.

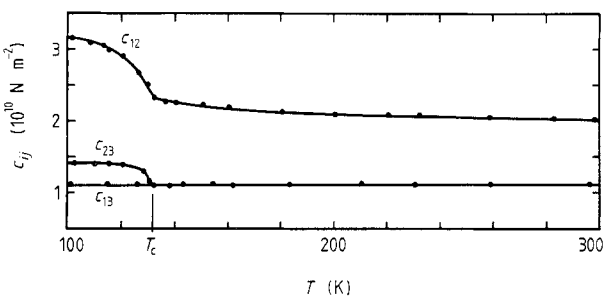

Figure 5. Temperature dependence of the c_{12}, c_{13} and c_{23} elastic constants.

Table 2. Elastic constants of LRSHS at 300, 132 (T_c) and 100 K (in units of 10^{10} N m^{-2}).

Elastic constant	Tetragonal phase (300 K)	T_c = 132 K	Orthorhombic phase (100 K)
c_{11}	3.80 ± 0.10	4.10	4.20
c_{22}	3.80	4.10	4.10
c_{33}	4.17	4.65	4.70
c_{44}	0.70 ± 0.07	0.70	0.72
c_{55}	0.70	0.70	0.70
c_{66}	0.45	0.08	0.22
c_{12}	2.00 ± 0.15	2.30	3.15
c_{13}	1.10	1.10	1.10
c_{23}	1.10	1.10	1.40

be affected by the piezoelectric correction. Using the temperature dependences of the piezoelectric moduli d_{ijk} and dielectric permittivity we estimate this correction to be less than 5%. Since experimental thermal expansion data for LRSHS are not available we could not estimate the isothermal contribution to the measured c_{11}, c_{22}, c_{33}, c_{12}, c_{13} and c_{23} elastic constants. However, the isothermal–adiabatic correction is generally of order 1–3% in these types of materials (Nye 1957). Taking this into account, together with the fact that the c_{66} elastic constant is related directly to the soft acoustic mode, which is not affected by any of these corrections, we will use the values of elastic constants calculated directly from the observed Brillouin line shifts, which are consistent with the accuracy of our measurements. We neglect the temperature dependence of crystal density and refractive indices for similar reasons.

4. Theoretical model

Based on the results described in the experimental part of this paper, it is assumed that e_6 is the spontaneous strain (henceforth denoted by e_s), which is either the primary (in the purely ferroelastic case) or a secondary (in the improper ferroelastic case) order parameter responsible for the structural phase transition under consideration. Figures 4 and 5 clearly demonstrate that virtually all the elastic coefficients c_{ij} are affected by the critical behaviour of e_s. Therefore, it can be deduced that there is significant coupling between the spontaneous strain e_s and the remaining components of the strain tensor e_i ($i = 1, 2, 3, 4, 5$). Figure 6 illustrates the temperature dependence of the dielectric polarisation and its square for the crystal in a broad temperature range around the critical temperature for this structural phase transition. The actual measurements of polarisation were obtained by integrating the pyroelectric coefficient, which was recently analysed in LRSHS (Wolejko *et al* 1988b) and involved a change of spontaneous polarisation ΔP_{exp}, and not its value in absolute units. These results indicate a very pronounced effect on ΔP_{exp} in the vicinity of the transition temperature $T \simeq 132$ K. A crossover from a square-root dependence on T at high temperatures ($T > T_c$) to a linear dependence on T at low temperatures ($T < T_c$) is quite apparent. It should be emphasised here that a transition from a non-polar to a polarised phase may take place at a much higher temperature, say T_p (possibly even above the melting point), and as such is not of immediate interest to us. The actual measurements of polarisation are reliable only up to 400 K since above that temperature the samples become conductive.

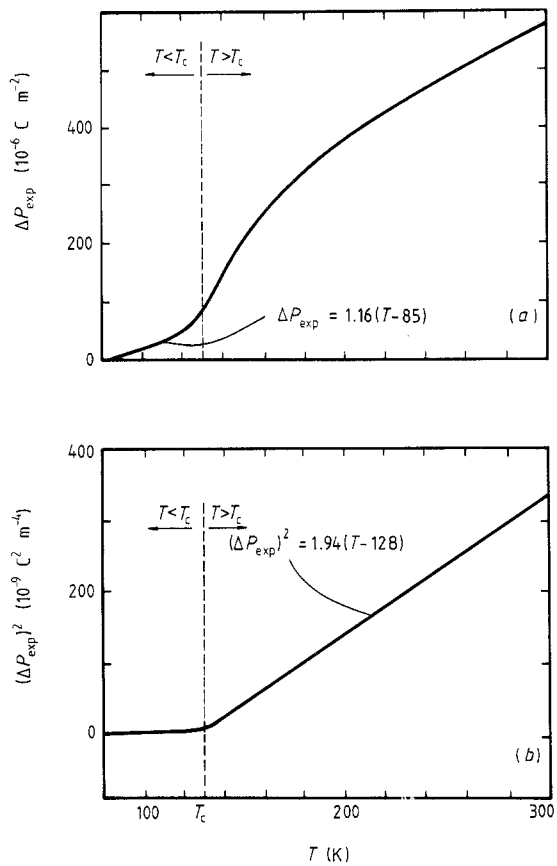

Figure 6. The temperature dependence of (*a*) measured polarisation ΔP_{exp} and (*b*) measured polarisation squared $(\Delta P_{exp})^2$ between 80 and 300 K, following the data of Wolejko *et al* (1988b) as per text.

The structural phase transition under consideration here appears to be of second order since calorimetric measurements (Wolejko *et al* 1988b) have not found evidence of latent heat of transition and the specific heat curve $C_p(T)$ shows no discontinuities but only a cusp at approximately 137 K. It is likely that the 5 K difference between T_c obtained using calorimetry and using Brillouin scattering can be attributed to different experimental techniques and their inaccuracies. Moreover, pyroelectric (Wolejko *et al* 1988b), dielectric (Wolejko *et al* 1988a) and scattering measurements (present paper) indicate no signs of thermal hysteresis effects or metastability.

Following the general approach to this problem outlined by Toledano *et al* (1983) and its specific applications such as those of Errandonea (1980), the appropriate phenomenological free-energy expansion can be written as follows

$$F = F_1(Q) + F_2(e_s, e_i) + F_3(P) + F_{12}(Q, e_s) + F_{23}(e_s, P) + F_{13}(Q, P) \tag{3}$$

where it has been assumed that Q is the primary order parameter for the transition, which transforms according to the irreducible representation E of the 4mm point group. As will become clear shortly, the assumption that e_6 is the primary order parameter (and thus that we deal with a purely ferroelastic transition) leads to a difficulty in explaining

the reduction in the slope of P as a function of T and the simultaneous incomplete softening of c_{66}. The terms of equation (3) are given as follows. The critical part is

$$F_1(Q) = (A_2/2)Q^2 + (A_4/4)Q^4 \tag{4}$$

where $A_2 = a(T - T_0)$, $A_4 > 0$, as required for a second-order transition. The term $F_2(e_s, e_i)$ is expanded to fourth order in elastic strains

$$F_2(e_s, e_i) = c^0_{2s}e_s^2 + \sum_{i\neq s} c^0_{ii}e_i^2 + \tfrac{1}{2}\sum_{\substack{i,j(\neq s)\\ i\neq j}} c^0_{ij}e_ie_j + \sum_{i(\neq s)} c^0_{3i}e_i^3$$
$$+ e_s^2 \sum_{i(\neq s)} c^0_{3is}e_i + \sum_{i,j,k(\neq s)} c^0_{ijk}e_ie_je_k + e_s^2 \sum_{i,j(\neq s)} c^0_{4ijs}e_ie_j + c^0_{4s}e_s^4 \tag{5}$$

where all the expansion coefficients are assumed constant so that the onset of criticality is brought about solely by $F_1(Q)$. Next, $F_3(P)$ is a fourth-order free-energy expansion of spontaneous polarisation

$$F_3(P) = B_2P^2 + B_4P^4 \tag{6}$$

where $B_2 = b(T - T_p)$, $b > 0$, $B_4 > 0$ and $T_p \gg T_c$. Close to T_p where P is virtually decoupled from other degrees of freedom, equation (6), through minimisation of $F_3(P)$, yields $P = 0$ for $T > T_p$ and a square-root dependence $P = P_s(T) \equiv \pm[-b(T - T_p)/2B_4]^{1/2}$ for $T \leqslant T_p$. Much below T_p, e.g. close to T_c, it is possible to expand $P_s(T)$ in a polynomial series

$$P_s(T) \simeq \pm[b(T_p - T_c)/2B_4]^{1/2}\left[1 + \frac{1}{2}\frac{T_c - T}{T_p - T_c} - \frac{1}{8}\left(\frac{T_c - T}{T_p - T_c}\right)^2 + \dots\right]. \tag{7}$$

In fact, since $T_c \ll T_p$ we can introduce the well known concept of molecular field (Jackson 1962) to replace higher-order non-linearities in the expansion of F_3 given by equation (6) so that a minimisation of F_3 with respect to P would produce the desired value of $P_s(T)$. Thus,

$$F_3 \simeq \tfrac{1}{2}\chi^{-1}P^2 - E_{\text{eff}}(T)P \tag{8}$$

where $P_s(T) = \chi E_{\text{eff}}(T)$ and χ is a mean-field dielectric coefficient of the sample.

The order parameter and spontaneous strain transform according to the same irreducible representation, so they are allowed to be coupled bilinearly such that

$$F_{12}(Q, e_s) = \mu Q e_s. \tag{9}$$

The lowest-order terms that are allowed, by symmetry principles, to reflect the couplings between polarisation and Q or e_s are biquadratic. Therefore,

$$F_{13}(Q, P) = (\nu/2)Q^2P^2 \tag{10}$$

and

$$F_{23}(e_s, P) = (\lambda/2)e_s^2P^2. \tag{11}$$

Minimisation of the free energy produces the following set of equations for the equilibrium values of the thermodynamic variables:

$$\partial F/\partial Q = A_2Q + A_4Q^3 + \mu e_s + \nu QP^2 = 0 \tag{12}$$

which implies that $e_s = 0$ whenever $Q = 0$. Then

$$\partial F/\partial P = \chi^{-1}P - E_{\text{eff}}(T) + \lambda e_s^2P + \nu Q^2P = 0 \tag{13}$$

which implies that $P = P_s(T)$ when $Q = e_s = 0$ and

$$P = P_s(T)/(1 + \lambda\chi e_s^2 + \nu\chi Q^2) \tag{14}$$

otherwise. Consequently, for the observed reduction in the slope of $P(T)$ below T_c, it must be required that $\lambda e_s^2 + \nu Q^2 > 0$. Next

$$\partial F/\partial e_s = \mu Q + 2e_s\left(c^0_{2s} + \sum_{i(\neq s)} c^0_{3is}e_i + \sum_{i,j(\neq s)} c^0_{4ijs}e_ie_j + (\lambda/2)P^2\right) + 4e_s^3c^0_{4s}. \tag{15}$$

Hence, the equilibrium value of e_s depends on couplings to other strain components and close to T_c is almost linearly dependent on Q. Finally

$$\partial F/\partial e_i = 2c^0_{ii}e_i + \sum_{j(\neq s)} c^0_{ij}e_j + 3c^0_{3i}e_i^2 + e_s^2c^0_{3is} + 3\sum_{j,k(\neq s)} c^0_{ijk}e_je_k + 2e_s^2\sum_{j(\neq s)} c^0_{4ijs}e_j = 0. \tag{16}$$

The second-order elastic coefficients are calculated in the usual way as

$$c_{ij} \equiv \partial^2F/\partial e_i\partial e_j = c^0_{ij} + 6\sum_{k(\neq s)} c^0_{ijk}e_k + 2e_s^2c^0_{4ijs} \tag{17}$$

$$c_{ii} \equiv \partial^2F/\partial e_i^2 = 2c^0_{ii} + 6c^0_{3i}e_i^2 \tag{18}$$

$$c_{is} \equiv \partial^2F/\partial e_i\partial e_s = 2e_s\left(c^0_{3is} + \sum_{j(\neq s)} c^0_{4ijs}e_j\right) \tag{19}$$

and

$$c_{2s} \equiv \partial^2F/\partial e_s^2 = 2c^0_{2s} + 12c^0_{4s}e_s^2 + \lambda P^2 + 2\left(\sum_{i(\neq s)} c^0_{3is}e_i + \sum_{i,j} c^0_{4ijs}e_ie_j\right). \tag{20}$$

4.1. The analysis above T_c (the actual transition temperature)

This is fairly simple. There, $Q = e_s = 0$ and $P = P_s(T)$. The experimentally measured polarisation, ΔP_{exp}, equals $\Delta P_{exp} = P_s - P_0$ in this particular temperature regime. Here P_0 is a reference polarisation. In our case $P_0 = P_s(T = 128\ \mathrm{K})$, as can be seen from the linear fit on the right-hand side of figure 6(*b*). Outside the immediate vicinity of T_c, figure 6(*b*) indicates that $(\Delta P_{exp})^2$ is a linear function of temperature. This may be at least roughly accounted for by a Taylor expansion of P_s given by equation (7). However, as we approach T_c from above, this approximation becomes less and less acceptable. We believe that in the immediate vicinity of T_c precursor effects come to play a major role in determining the form of $\Delta P_{exp}(T)$. More specifically, through equation (14) and the fact that $Q = e_s = 0$ at $T > T_c$ one could approximate

$$P_{exp} \simeq \frac{P_s(T)}{(1 + \lambda\chi\langle e_s^2\rangle + \nu\chi\langle Q^2\rangle)} - P_0 \tag{21}$$

where $\langle e_s^2\rangle$ and $\langle Q^2\rangle$ are the mean values of critical fluctuations of the spontaneous strain and the order parameter, respectively. It is well known that these quantities increase dramatically as the critical temperature is approached. In fact, at T_c, $\langle Q^2\rangle$ should diverge with a critical exponent -1 (using Gaussian approximation), i.e. $\langle Q^2\rangle \propto (T - T_c)^{-1}$. Thus, it is seen from equation (21) that the closer we get to T_c the more dominant is the role of critical fluctuations in the form of P_{exp} (precursor effects). A more detailed analysis of this effect is intended in the near future.

Furthermore, neglecting third- and fourth-order mode–mode coupling in equation (16), multiplying the equation on both sides by the compliance tensor s^0_{ij} and summing over i allows us to solve it for the remaining strain components:

$$e_i = 0 \qquad \text{or} \qquad e_i \simeq -2c^0_{ii}/3c^0_{3i} \equiv e_i^0. \tag{22}$$

At present, no x-ray or thermal expansion data are available that could indicate if any

Table 3. Numerical values of the thermal expansion parameters for the second-order elastic coefficients c_{ij}, c_{ii} and c_{2s} (in units of 10^{10} N m^{-2}).

Elastic coefficient	$T > T_c$	$T \leqslant T_c$	$T \leqslant T_c$
c_{11}	$\alpha_{11} = \alpha_{22} = 4.1$	$\alpha_{11} = 4.1$	$\beta_{11} = 3.13 \times 10^{-3}$
c_{22}		$\alpha_{22} = 4.1$	$\beta_{22} = 0.0$
c_{33}	$\alpha_{33} = 4.65$	$\alpha_{33} = 4.65$	$\beta_{33} = 1.56 \times 10^{-3}$
c_{44}	$\alpha_{44} = \alpha_{55} = 0.70$	$\alpha_{44} = 0.70$	$\beta_{44} = 0.63 \times 10^{-3}$
c_{55}		$\alpha_{55} = 0.70$	$\beta_{55} = 0.0$
c_{66}	$\alpha_{66} = 0.098$ $\beta^{+}_{66} = 3.7 \times 10^{-3}$ $\gamma^{+}_{66} = -0.99 \times 10^{-5}$	$\alpha_{66} = 0.08$ $\gamma^{-}_{66} = -6.24 \times 10^{-5}$	$\beta^{-}_{66} = 6.03 \times 10^{-3}$
c_{12}	$\alpha_{12} = 2.27$	$\alpha_{12} = 2.33$ $\gamma_{12} = -9.9 \times 10^{-4}$	$\beta_{12} = 5.62 \times 10^{-2}$
c_{23}	$\alpha_{23} = \alpha_{13} = 1.10$	$\alpha_{23} = 1.12$ $\gamma_{23} = -6.63 \times 10^{-4}$	$\beta_{23} = 2.82 \times 10^{-3}$
c_{13}		$\alpha_{13} = 1.10$ $\gamma_{13} = 0.0$	$\beta_{13} = 0.0$

strain components are in fact non-zero, but this possibility cannot be excluded *a priori*. Then, using equations (17)–(20) we readily find the elastic coefficients as

$$c_{ij} = \alpha_{ij} \qquad c_{ii} = \alpha_{ii} \qquad c_{is} = 0 \tag{23}$$

all of which are constant, and

$$c_{2s} = \alpha_{2s} + \beta^{+}_{2s}(T - T_c) + \gamma^{+}_{2s}(T - T_c)^2 \tag{24}$$

where all the parameters are displayed in the Appendix. The experimentally determined values of these parameters have been summarised in table 3 both for $T > T_c$ and for $T \leqslant T_c$. Once the experimental data for $e^0_i(T)$ become available, we will be able to calculate the values of the expansion coefficients of the free energy using the formulae given in the Appendix.

4.2. *The analysis below* T_c

This is more complicated. First of all, since this is a second-order transition and calculations are done in the mean-field approximation, we have

$$e_s \simeq d_s(T_c - T)^{1/2} \qquad Q$$
$$\simeq d_Q(T_c - T)^{1/2} \tag{25}$$

provided T is sufficiently close to T_c. Both T_c and the coefficients d_s and d_Q will be subject to further determination. Then, assuming some simplifying conditions (Mróz *et al* 1987), namely

$$2c^0_{ii}e_i + \sum_{j(\neq s)} c^0_{ij}e_j \simeq g_1 = \text{const} \tag{26a}$$

$$\sum_{j(\neq s)} c^0_{4ijs}e_j \simeq g_2 = \text{const} \tag{26b}$$

$$\sum_{j,k(\neq s)} c^0_{ijk} e_j e_k \simeq 0 \tag{26c}$$

from equation (16) we obtain a simple equation relating e_i and e_s yielding

$$e_i \simeq [(e_i^0)^2 + \delta_i(T_c - T)]^{1/2} \tag{27}$$

where $\delta_i = -d_s^2(c^0_{3is} + 2g_2)/3c^0_{3i}$ and $e_i(T)$ is subject to further experimental verification once relevant data become available. Substituting equations (25) and (7) into equations (12) and (13) yields approximate expressions for d_Q and d_s:

$$d_Q \simeq a - (b\nu/2B_4) \tag{28a}$$

$$d_s \simeq -\mu d_Q \Big/ 2\Big(c^0_{2s} + \sum_{i\neq s} e_i^0(c^0_{3is} + g_2) - \lambda b(T_p - T_c)/4B_4\Big). \tag{28b}$$

To derive an approximate expression for spontaneous polarisation below T_c we use equation (14) where we substitute the expansion of $P_s(T)$ around T_c, i.e. equation (7), and insert the relevant formula for e_s and Q, i.e. equation (25). This yields for the experimentally observed polarisation

$$\Delta P_{exp} = P(T) - P_0 \simeq P_s^c[1 + p_1(T_c - T) + \ldots] - P_0 \tag{29}$$

where $P_s^c = P_s(T_c)$ and $p_1 = \frac{1}{2}(T_p - T_c)^{-1} - \lambda\chi d_s - \nu\chi d_Q$. This indeed gives a straight line as shown on the left-hand side of figure 6(*a*) and it also agrees with respect to the reduction in the slope of $P(T)$ below T_c as compared to the tangent line just above T_c.

Furthermore, second-order elastic coefficients are found as follows:

$$c_{ij} \simeq \alpha_{ij} + \beta_{ij}(T_c - T) + \gamma_{ij}(T_c - T)^2 + \ldots \tag{30}$$

$$c_{ii} \simeq \alpha_{ii} + \beta_{ii}(T_c - T) + \ldots \tag{31}$$

$$c_{is} = 2d_s(T_c - T)^{1/2}\Big(c^0_{3is} + \sum_{j(\neq s)} c^0_{4ijs}[(e_j^0)^2 + \delta_j(T_c - T)]^{1/2}\Big) \tag{32}$$

and

$$c_{2s} = \alpha_{2s} + \beta^-_{2s}(T_c - T) + \gamma^-_{2s}(T_c - T)^2 \tag{33}$$

where all the parameters have been explicitly displayed in the Appendix and their numerical values given in table 3. Since the off-diagonal coefficients c_{ij} contain a term proportional to e_s^2 and another proportional to e_k while the diagonal ones c_{ii} do not depend directly on e_s but only on e_i^2, it is expected that the former ones (c_{ij}) exhibit a more curved temperature dependence while the latter ones (c_{ii}) are fairly linear functions of temperature. This is, in fact, borne out experimentally as shown by the results presented in figures 4 and 5. In addition, we find that c_{12}^2 and c_{23}^2 are straight lines within $|\varepsilon| = 0.1$, lending credence to our assumption about the square-root behaviour of e_i as given by equation (27). Moreover, it is clear that, sufficiently close to T_c, c_{2s} is an almost linear function of $(T_c - T)$ as shown in figure 7. However, for temperatures further removed from T_c, a quadratic non-linearity becomes noticeable as shown in figure 4.

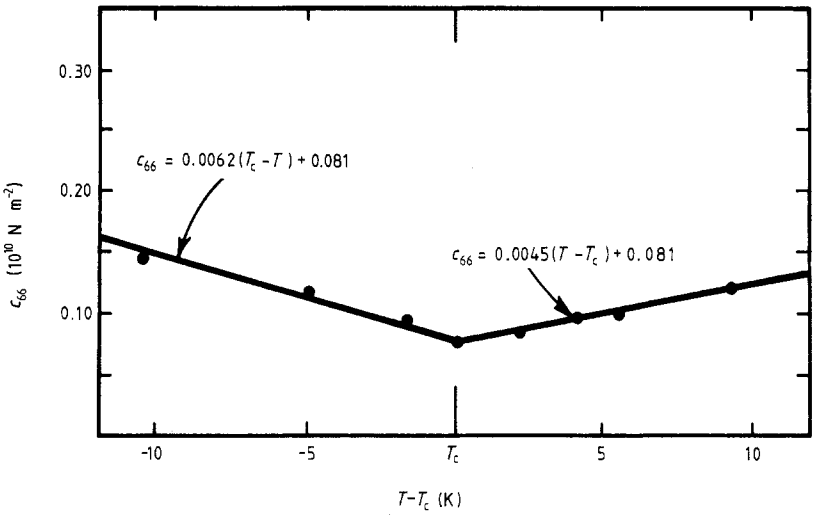

Figure 7. A close-up view of the temperature dependence of c_{2s} in the vicinity of T_c.

It is also easy to see that, because of the coupling with polarisation, c_{2s} exhibits an incomplete softening as $T \rightarrow T_c$. The condition on the transition temperature T_c can be derived from the instability condition on F, i.e. $\delta^2 F = 0$, as

$$a(T_c - T_0)[\alpha_{2s}^0 + \lambda b(T_p - T_c)/2B_4] = \mu^2 \tag{34}$$

which is a quadratic equation for T_c and we have denoted

$$\alpha_{2s}^0 \equiv 2c_{2s}^0 + 2\left(\sum_{i(\neq s)} c_{3is}^0 e_i^0 + \sum_{i,j(\neq s)} c_{4ijs}^0 e_i^0 e_j^0\right).$$

We also have $a > 0$, $\alpha_{2s}^0 > 0$, $B_4 > 0$ and $T_p > T_c$. Since $c_{2s} > 0$ for $T > T_c$ and it decreases as $T \rightarrow T_c$ from above, it is implied that $\lambda < 0$ (while $\nu > 0$ in equation (14) to give the proper behaviour of $P(T)$). Consequently, we see from equation (34) that $T_c > T_0$. Hence, it follows from equation (23) that

$$c_{2s}(T_c) = \mu^2/a(T_c - T_0) > 0 \tag{35}$$

as required by experiment.

5. Conclusions

In this paper we have presented the results of our experimental high-resolution Brillouin spectroscopy studies of the elastic properties of the ferroelastic $LiRb_5(SO_4)_3 \cdot 1.5H_2SO_4$ crystal. From the velocities of 12 acoustic modes we have found the temperature behaviour of all non-zero components of the elastic stiffness tensor in the range from 100 to 300 K. In particular, the c_{66} elastic constant corresponding to the soft mode of this para- to ferroelastic phase transition was found to decrease to a non-zero minimum as $T \rightarrow T_c \simeq$ 132 K. Also, most of the other elastic constants were substantially affected by the onset of the transition. In the second part of the paper we have presented a theoretical model based on a Landau-type free-energy expansion involving the order parameter Q, strain components e_s and e_i, and polarisation P. It has been demonstrated that assuming a

pseudo-proper character of this ferroelastic phase transition one can consistently account for all the main experimental features, i.e. the temperature behaviours of c_{ii}, c_{ij} and c_{2s} both above and below T_c, especially the incomplete softening of c_{2s} at T_c, as well as the crossover of the polarisation's dependence on temperature from a square-root to a nearly linear function.

It should be emphasised that for internal consistency of the derivation (agreement with experiment) is was crucial that e_s was coupled to *both* Q and P. If only a bilinear coupling between e_s and Q were to be included one could not possibly expect an incomplete softening of c_{2s}. Thus, the coupling between spontaneous strain and polarisation (as a result of $P \neq 0$ at and around T_c) makes the elastic part of the system show incomplete softening. On the other hand, neither polarisation nor spontaneous strain can be considered a primary order parameter in this transition. The transition is driven by Q. Therefore, all the three parameters and couplings between them are necessary to account for all the observed effects.

The predicted temperature dependences of the spontaneous strain and other strain components should be verified experimentally using x-ray measurements in the near future. This would greatly help in a more quantitative analysis of the transition since one could then extract all the parameters (or at least the most dominant ones) of the theory.

The measurements of the soft mode were carried out on three different samples cut from two different crystals. The accuracy of the cut was 0.2°, and hence the authors exclude the inaccuracy of the cut as a possible reason for the incomplete mode softening observed for c_{2s}. One could speculate on other mechanisms which may take place during the discussed transition. It might be envisaged that the low-temperature phase is not mm2, in which case the actual soft phonon does not propagate along one of the investigated directions. Another possibility is that e_s is coupled to the fluctuations of the order parameter or that one of the phases is incommensurate. As of now, however, there exist no experimental indications to support such ideas. Consequently, we have presented the most feasible scenario which would be compatible with the experimental data.

Acknowledgments

Three of the authors (JAT, HK and MJC) express their gratitude to the Natural Sciences and Engineering Research Council of Canada for the financial support of this project. One of the authors (BM) wishes to thank the faculty and staff of the Department of Physics at Memorial University of Newfoundland for their hospitality during his stay in St John's.

Appendix. Second-order elastic coefficients

For $T > T_c$ we have

$$\alpha_{ij} = c_{ij}^0 + 6 \sum_{k(\neq s)} c_{ijk}^0 e_k^0 \tag{A1}$$

$$\alpha_{ii} = 2c_{ii}^0 + 6c_{3i}^0 (e_i^0)^2 \tag{A2}$$

$$\alpha_{2s} = 2c_{2s}^0 + 2\left(\sum_{i(\neq s)} (c_{3is}^0 + g_2) e_i^0 \right) + \lambda (P_s^c)^2 \tag{A3}$$

$$\beta_{2s}^{+} = -\lambda P_s^c/2(T_p - T_c) \tag{A4}$$

$$\gamma_{2s}^{+} = -\lambda P_s^c/8(T_p - T_c)^2. \tag{A5}$$

For $T < T_c$ we have α_{ij} which is that of equation (A1) and

$$\beta_{ij} = 3\sum_{k(\neq s)} (c_{ijk}^0 \delta_k / e_k^0) + 2c_{4ijs}^0 d_s^2 \tag{A6}$$

$$\gamma_{ij} = -\tfrac{3}{4}\sum_{k(\neq s)} c_{ijk}^0 \delta_k^2/(e_k^0)^3 \tag{A7}$$

where the summation is only over k for which $e_k^0 \neq 0$. α_{ii} is that of equation (A2) and

$$\beta_{ii} = 3c_{3i}^0 \delta_i / e_i^0. \tag{A8}$$

α_{2s} is that of equation (A3) and

$$\beta_{2s}^{-} = 12c_{4s}^0 d_s^2 + \sum_{i(\neq s)} (g_2 + c_{3is}^0)\delta_i/e_i^0 + 2\lambda(P_s^c)^2 p_1 \tag{A9}$$

$$\gamma_{2s}^{-} = -\sum_{i(\neq s)} [(g_2 + c_{3is}^0)\delta_i^2/4(e_i^0)^3] + \lambda (P_s^c)^2 p_1^2. \tag{A10}$$

References

Ahmad S F, Kiefte H, Clouter M J and Whitmore M 1982 *Phys. Rev.* B **26** 4239

Brugger K 1965 *J. Appl. Phys.* **36** 759

Cummins H Z 1983 *Light Scattering Near Phase Transitions* ed. H Z Cummins and A P Levanyuk (Amsterdam: North-Holland)

Errandonea G 1980 *Phys. Rev.* B **21** 5221

Jackson J D 1962 *Classical Electrodynamics* 2nd edn (New York: Wiley)

Landau L D and Lifshitz E M 1959 *Theory of Elasticity* (New York: Addison-Wesley)

Mróz B, Kiefte H and Clouter M J 1988 *Ferroelectrics* **82** 105

Mróz B, Kiefte H, Clouter M J and Tuszyński J A 1987 *Phys. Rev.* B **36** 3745

Mróz B, Tuszyński J A, Kiefte H and Clouter M J 1989 *J. Phys.: Condens. Matter* **1** at press

Nye J F 1957 *Physical Properties of Crystals* (Oxford: OUP)

Pietraszko A 1987 private communication

Toledano P, Fejer M M and Auld B A 1983 *Phys. Rev.* B **27** 5717

Vacher R and Boyer L 1972 *Phys. Rev.* B **6** 639

Vacher R, Boyer L and Boissier M 1972 *Phys. Rev.* B **6** 674

Wadhawan V K 1982 *Phase Transitions* **3** 3

Wolejko T, Pakulski G and Tylczyński Z 1988a *Ferroelectrics* **81**

Wolejko T, Piskunowicz P, Breczewski T and Krajewski T 1988b *Ferroelectrics* **81**